

Elucidation of Metabolite Markers for Medulloblastoma Metastasis with Three-Dimensional Mass Spectrometry Imaging

Paine, M.R.L.^{1,2}; Liu, J.³; Ellis, S.R.²; Trede, D.⁴; Kobarg, J.H.⁴; Heeren, R.M.A.²; Fernández, F.M.¹; MacDonald, T.J.¹

¹Georgia Institute of Technology, Atlanta, GA; ²Maastricht Multimodal Molecular Imaging (M4I) Institute, Maastricht, Netherlands; ³Emory University School of Medicine, Atlanta, GA; ⁴SCILS, Bremen, Germany

Introduction

- Medulloblastoma (MB) is most common malignant brain tumor of children. Presence of metastasis is most robust predictor of mortality.
- We employ a mass spectrometry imaging (MSI) approach in a mouse model to elucidate key metabolome differences associated with metastasis for high-risk sonic hedgehog-activated subgroup (SHH MB).
- Expansion to three-dimensional MSI provides an closer representation of the underlying biological heterogeneous structure.
- We identified metabolites differentially expressed in metastasizing tumors compared with non-metastasizing tumors.
- They provide better understanding of tumor progression. They could lead to diagnostic biomarkers and targets for prevention of metastasis.

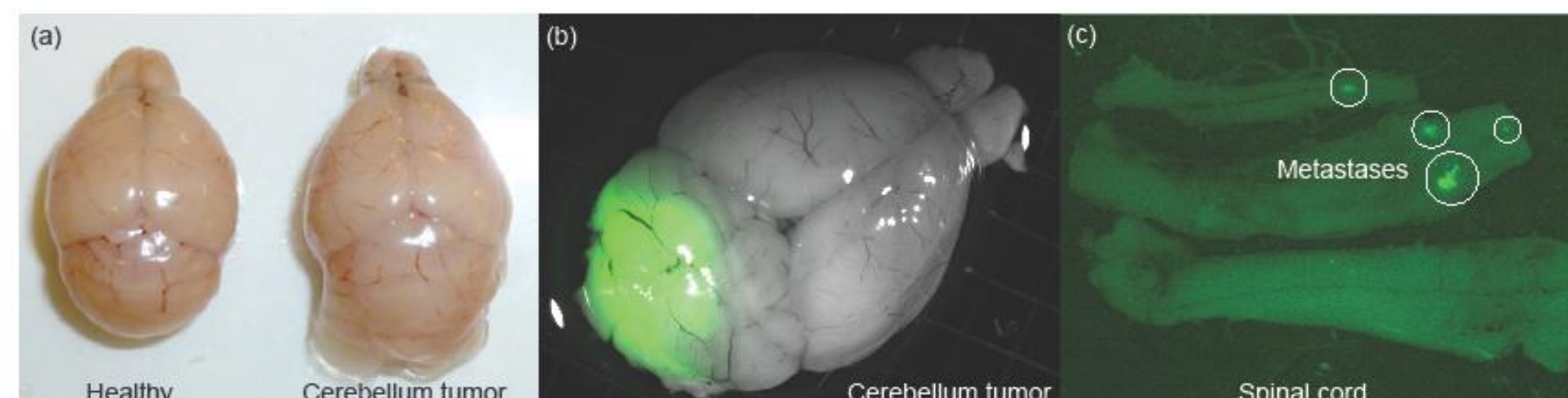


Figure 1: (a) Optical image of healthy brain and brain containing a cerebellum tumor. (b) Primary tumor visualized using fluorescence microscopy (GFP). (c) Positive identification of a metastasizing primary tumor by visualizing the metastases in the spinal cord with the detection of GFP (white circles) using fluorescence microscopy.

Methods

- After mice were sacrificed, brains and spinal cords were removed and inspected using fluorescence microscopy to classify tumors as metastasizing or non-metastasizing (Fig. 1). 3 brains identified as non-metastasizing tumor, 3 brains containing a metastasizing tumor.
- For each brain 30–50 tissue sections were cut and mounted on ITO slides. Norharmane matrix has been coated using TM-Sprayer (HTX).
- Tissue sections were analyzed in negative-ion mode using a MALDI ToF mass spectrometer (rapifleX, Bruker) operating in reflectron mode. Spectra were acquired in the m/z 400–1600 range at 50 μm² pixels.
- In total, 223 sections were analyzed (105 from non-metastasizing, 118 from metastasizing tumor) totaling 10.2 million spectra (3.3 TB).
- For annotation of anatomical regions, 3D spatial segmentation by means of statistical clustering was performed. This allowed to delineate regions corresponding to white matter, grey matter, primary tumor.
- To find m/z markers discriminating metastasizing and non-metastasizing primary tumors, we used receiver operating characteristic (ROC).

Results

- 3D models were constructed by rigid registration based on spatial distribution of ions at m/z 885.5 (Fig. 2). Spatial segmentation has been applied to identify 3D tumor volumes (Fig. 3). Segments were validated against multiple H&E stained sections by a trained histopathologist (Fig. 4).
- Average mass spectra were created for the three major regions (Fig. 5). The contrasting tumor lipidome is what differentiates the tumor region from the remainder tissue. Comparing both tumor region mean spectra (Figs. 5c and f) does not immediately reveal observable differences. Therefore individual mass spectra from non-metastasizing and metastasizing tumors were statistically compared by means of ROC analysis.
- For ROC analysis, 441,152 spectra from non-metastasizing and 1,010,805 spectra from metastasizing tumor regions were compared. Signals having AUC ≥0.6 were deemed significantly decreased in the metastasizing tumor while signals having AUC ≤0.4 were significantly increased. Using these thresholds, 10 metabolites (6 decreased, 4 increased) were identified as having significant differences in TIC normalized abundances (Tab. 1). Extracted-ion images for these metabolites within the tumor region are shown in Fig. 6 for a single section chosen at random from each brain.
- For each metabolite, a heterogeneous spatial distribution in 3-dimensions was observed throughout the tumor volume, particularly for those at low abundances. This observation illustrates the crucial importance of 3D-MSI for accurate identification of biologically relevant metabolites.
- Assignment of chemical structures to the discriminant markers was accomplished using accurate mass measurements and MS/MS experiments.
- The six decreased species included two phosphatidic acids (PA), three phosphatidylethanolamines (PE), and a phosphatidylserine (PS). Several studies have identified PAs as overexpressed in tumor metastasis. Our observations of decreased PAs are seemingly contrary to these findings.
- Among the four metabolites increased in metastasizing tumors are a phosphatidylinositol (PI) and two phosphoinositides (PIP). The PIPs are involved in the survival and growth of normal cells. Dysregulation of the corresponding pathway has been widely associated with oncogenesis in humans. Elevation of the identified PIP's in metastasizing tumors provides strong evidence that the pathway is upregulated in metastasizing tissue.

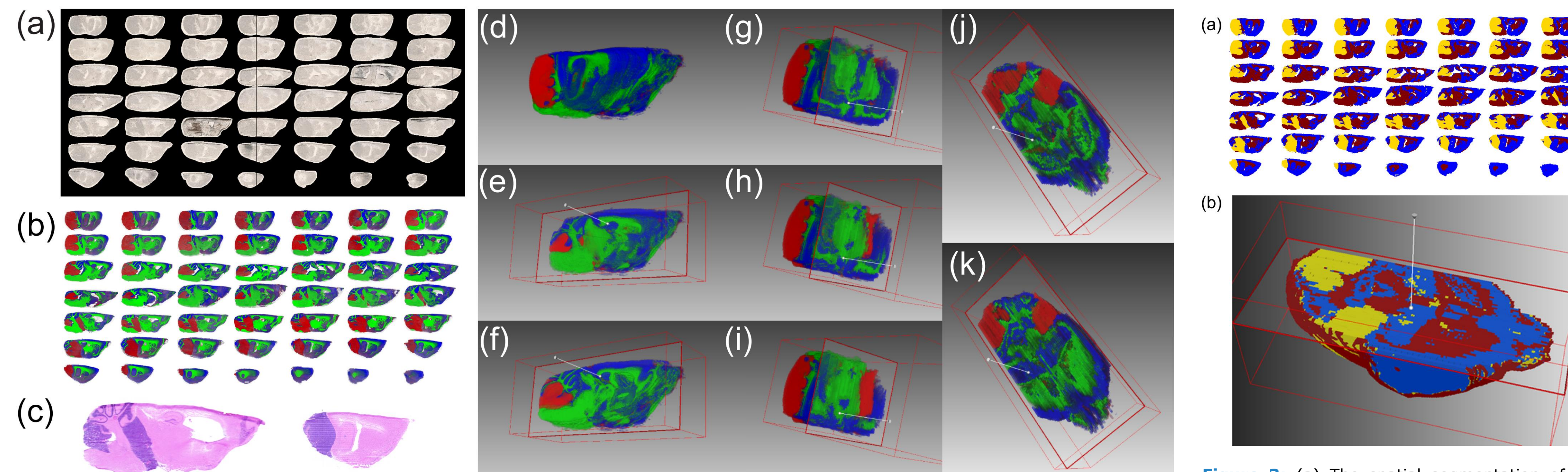


Figure 3: (a) The spatial segmentation of a brain containing a non-metastasizing tumor showing clear delineation of healthy tissue (blue, red) and the primary tumor (yellow). (b) Visualization of the segmentation map in 3D as a transverse virtual section. (c) Optical images of the 49 sections from a mouse brain containing a non-metastasizing tumor with (b) the corresponding MS visualization using three representative channels; m/z 790.5 blue, m/z 888.6 green, and m/z 885.5 red. (d) H&E stains of sections no. 29 and 41. (e-f) Two sagittal, (g-i) three coronal, and (j-k) two transversal virtual sections.

Conclusion

- With a 3D-MSI approach, we identified 10 metabolites that are differentially expressed within non-metastasizing and metastasizing SHH MB primary tumors. Due to the low abundance and heterogeneity of metabolites, elucidation was only successful by 3D imaging of the brain.
- The identified metabolites represent candidates for validation and for further functional investigation.
- Whether these metabolites are specific to SHH MB metastasis, or MB metastasis in general, will also need to be verified in future studies.

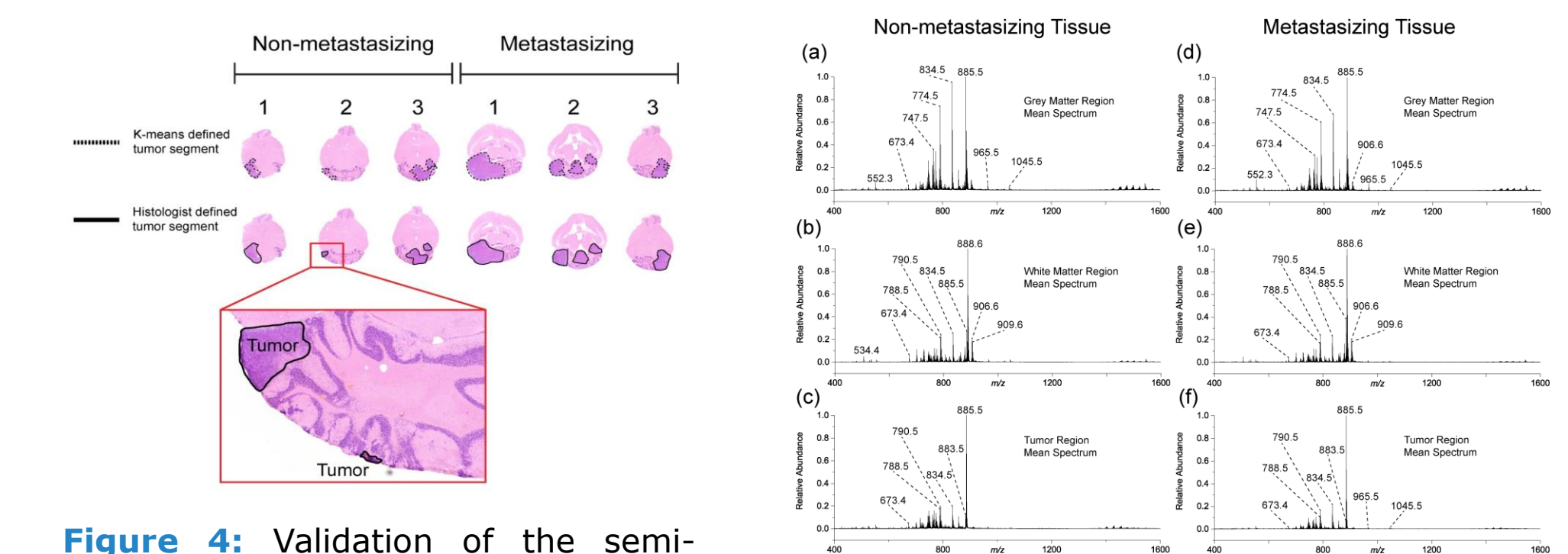


Figure 4: Validation of the semi-supervised spatial segmentation by comparison with histological annotation of the H&E stained tumor tissue.

Figure 5: Mean spectra for grey matter, white matter, and tumor regions in a non-metastasizing primary tumor (a-c) and metastasizing (d-f) primary tumor.

Measured m/z	Theo. m/z	Mass accuracy (ppm)	AUC value	Assigned Metabolite
Decreased in metastasizing tissue				
673.4811	673.4814	0.4	0.65	PA(16:0_18:1)
723.4968	723.4968	0.05	0.69	PA(18:0_20:4)
726.5440	726.5443	0.4	0.61	PE(P-18:1/18:1)
				PE(O-18:2/18:1)
738.5078	738.5079	0.1	0.64	PE(16:0_20:4)
742.5390	742.5392	0.3	0.66	PE(18:1/18:1)
760.5131	760.5134	0.4	0.67	PS(16:0_18:1)
Increased in metastasizing tissue				
834.5284	834.5291	0.8	0.40	PS(18:0_22:6)
885.5489	885.5499	1.1	0.31	PI(18:0_20:4)
965.5155	965.5156	0.1	0.37	PIP(18:0_20:4)
1045.4812	1045.4820	0.8	0.36	PIP(18:0_20:4)

Table 1: Differential metabolites identified in [M-H]⁻ ionic species.

Acknowledgements

The authors acknowledge the American Society for Mass Spectrometry for the Post-doctoral Research Award to MRLP that made this collaboration possible. Math3-GFP reporter mice were kindly provided by Dr. Tracy-Ann Read (Emory Winship Cancer Institute). The authors also acknowledge Matthew Schindler (Emory University School of Medicine) for graciously agreeing to perform an independent neuropathology review of the mice brain tissue. PNF thanks support from endowed Vasser-Woolley funds, and from the Emory/Georgia Tech/Children's Healthcare of Atlanta Center for Pediatric Nanomedicine. Part of this research has been made possible with the support of the Dutch Province of Limburg. Part of the research performed by Maastricht University has been funded by ITEA and RVO (project numbers ITEA151003/ITEA 14001).

Figure 6: H&E stained sections for each of the 6 mouse brains and corr. extracted-ion images for 10 identified metabolites.